JOURNAL OF PHYSICAL ORGANIC CHEMISTRY
J. Phys. Org. Chem. 2002; **15:** 660–666
Published online in Wiley InterScience (www.interscience.wiley.com). DOI: 10.1002/poc.529

Density functional theory study of the Lewis acid-catalyzed Diels–Alder reaction of nitroalkenes with vinyl ethers using aluminum derivatives

Luis R. Domingo,* Amparo Asensio and Pau Arroyo

Instituto de Ciencia Molecular, Departamento de Química Orgánica, Universidad de Valencia, Dr. Moliner 50, E-46100 Burjassot, Valencia, Spain

Received 5 March 2002; revised 11 April 2002; accepted 18 April 2002

ABSTRACT: The inverse electron demand Diels–Alder reaction of nitroalkenes with vinyl ethers catalyzed by Lewis acids based on aluminum metal, $AlMe_3$, $Al(OMe)_3$ and $AlCl_3$ was studied using density functional theory methods. A continuum model was selected to represent the effects of dichloromethane used as solvent. For this cycloaddition reaction two reactive channels corresponding to the *endo* and *exo* approach modes of the vinyl ether to the Lewis acid-coordinated nitroalkene were studied. Coordination of the aluminum metal to an oxygen atom of the nitroalkene increases the electrophilicity of the heterodiene, decreasing the activation energy of the cycloaddition. The substitution effect on the aluminum metal with Me, OMe and Cl on the activation energy and the stereoselectivity is discussed. An analysis of the static electrophilicity on reactants allows an explanation of the behavior of these Lewis acid-catalyzed cycloadditions. Copyright © 2002 John Wiley & Sons, Ltd.

KEYWORDS: density functional theory; Lewis acid catalysis; Diels–Alder reaction; nitroalkenes; vinyl ethers; aluminum catalysts

INTRODUCTION

The Diels–Alder (DA) reaction is one of the most useful synthetic reactions and its overwhelming importance is well known and thoroughly documented in organic chemistry. Its usefulness arises from its versatility and its remarkable selectivity; many synthetic routes to cyclic compounds are made possible through DA reactions, which can involve a large variety of dienes and dienophiles.[1] Lewis acid (LA) catalysts considerably extend the useful scope of the DA reaction, enhancing the reaction rate and leading to significant changes in *endo/exo* and regio selectivities in comparison with the uncatalyzed process.[2]

Both normal and inverse electron demand (IED) DA reactions involving oxygenated reagents can be catalyzed in the presence of LAs. The coordination of an electron-deficient DA reagent to a LA increases notably the electrophilicity of the former. The enhanced reactivity has been simulated in many theoretical studies.[3] Recently we have studied the IED Diels–Alder reaction of nitroalkenes with electron-rich dienophiles.[4] Thus, whereas enamines acting as strong nucleophiles react easily with simple nitroalkenes, vinyl ethers normally need the presence of a LA in order to make the cycloaddition feasible.[5] Experimentally, bulky LAs based on aluminum derivatives such as methylaluminum bis(2,6-dimethylphenoxide) (MAPh) and methylaluminum bis(2,6-di-tert-butyl-4-methylphenoxide) (MAD) are used in order to enhance the rate and stereoselectivity.[5] However, the large molecular system for these bulky LA catalysts prevents an *ab initio* study (see the **R1**-MAPh complex in Fig. 1). Although semiempirical calculations can be done for these systems[4a], the limitations and weakness of the semiempirical methods for analyzing this type of chemical reactions have been emphasized.[6] In consequence, BH_3 has been widely used as a computational model for these LA-catalyzed DA reactions.[4b,c]

In this work, the LA-catalyzed DA reaction of nitroethene, **R1**, with methyl vinyl ether (MVE), **R2**, using three aluminum derivatives [$AlMe_3$, $Al(OMe)_3$ and $AlCl_3$] as LA catalysts was studied using density functional theory[7] (DFT) methods in order to elucidate the substitution effect on the aluminum metal on both reactivity and steroselectivity. The results are compared with those obtained using BH_3 as a computational model.[4b,c] Solvent effects were also considered in order to elucidate the role of the solvent in these LA-catalyzed cycloadditions.

**Correspondence to:* L. R. Domingo, Instituto de Ciencia Molecular, Departamento de Química Orgánica, Universidad de Valencia, Dr. Moliner 50, E-46100 Burjassot, Valencia, Spain.
E-mail: domingo@utopia.uv.es
Contract/grant sponsor: Ministerio de Educación y Cultura.
Contract/grant sponsor: DGICYT; *Contract/grant number:* PB98-1429.

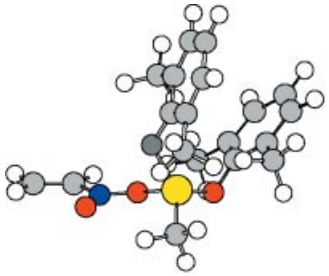

Figure 1. R1-MAPh complex

COMPUTATIONAL METHODS

DFT calculations were carried out using the B3LYP[8] exchange-correlation functional, together with the standard 6–31G* basis set.[9] The optimizations were carried out using the Berny analytical gradient optimization method.[10] The stationary points were characterized by frequency calculations in order to verify that the transition structures have one and only one imaginary frequency.[11] The intrinsic reaction coordinates[12] (IRC) paths were traced in order to check the energy profiles connecting each transition structure to the two associated minima of the proposed mechanism by using the second-order González–Schlegel integration method.[13] The electronic structures of stationary points were analyzed by the natural bond orbital (NBO) method.[14] All calculations were carried out with the Gaussian 98 suite of programs.[15] Optimized geometries of all structures are available from the authors.

The solvent effects were treated by B3LYP/6–31G* single-point calculations at the gas-phase stationary points involved in the reaction using a relatively simple self-consistent reaction field[16] (SCRF) based on the polarizable continuum model (PCM) of Tomasi's group.[17] Since the solvent used is usually dichloromethane, we used the dielectric constant at 298.0 K of $\varepsilon = 8.93$.

The global indexes defined in the context of the DFT,[18,19] the electronic chemical potential μ, chemical hardness η and electrophilicity power ω values were approximated in terms of the one electron energies of the frontier molecular orbitals (FMO) HOMO and LUMO, ε_H and ε_L, using the expressions $\mu \approx (\varepsilon_H + \varepsilon_L)/2$, $\eta \approx \varepsilon_L - \varepsilon_H$ and $\omega = \mu^2/2\eta$, respectively, at the ground state (GS) of the molecules (see Refs 20 and 21 for more detailed information).

RESULTS AND DISCUSSION

Energies

The cycloaddition reaction between the LA-coordinated nitroethenes **R1-X** (**X** = Me for $AlMe_3$, **X** = OMe for $Al(OMe)_3$ and **X** = Cl for $AlCl_3$) and vinyl methyl ether **R2** can take place along four reaction pathways because of the asymmetry of both reactants. They are related with the *endo* and *exo* stereoisomeric and *ortho* (head-to-head) and *meta* (head-to-tail) regioisomeric reactive channels. Previous theoretical studies devoted to these cycloadditions have shown that they present a large *ortho* regioselectivity.[4] Therefore, only the *endo* and *exo* reactive channels along the more favorable *ortho* approach mode of MVE to **R1-X** were considered (see Scheme 1). Analysis of the results indicates that these cycloadditions are concerted processes associated with highly asynchronous transition states (TSs). Thus two TSs, **TS-en-X** and **TS-ex-X**, corresponding to the *endo* and *exo* approach modes along the *ortho* regioisomeric channel were found and characterized for each of these LA-catalyzed cycloadditions. From the TSs the related minima associated with the final cycloadducts can be obtained, the *endo* and *exo* cycloadducts **P-en-X** and **P-ex-X**. Some selected geometric parameters of the calculated TSs are shown in Fig. 2 and Table 1 reports the values of the total and relative energies for the stationary points. For MVE an s-*trans* conformation of

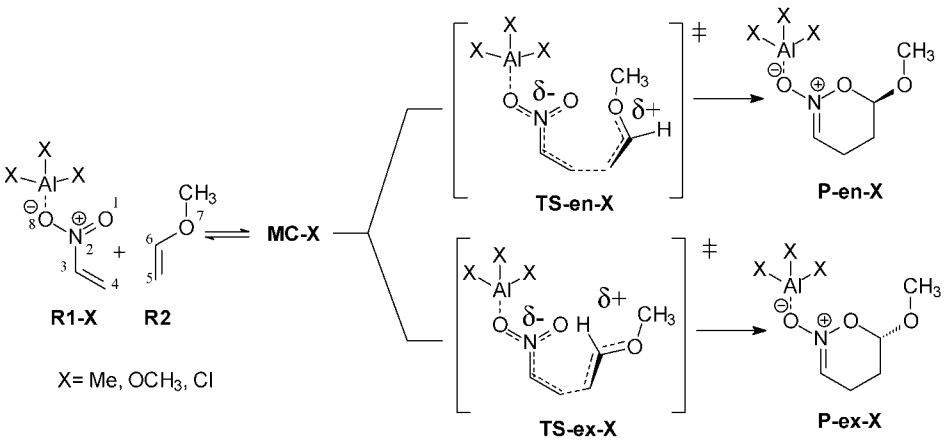

Scheme 1

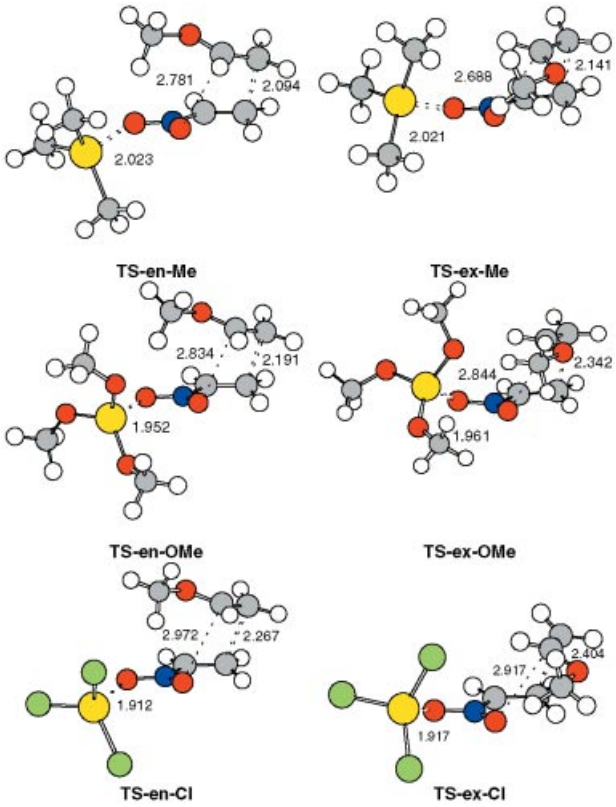

Figure 2. Transition structures corresponding to the LA aluminum-catalyzed reaction between nitroethene **R1** and the enol ether **R2**. The values of the bond lengths directly involved in the process are given in ångstroms

the methyl group with respect to the vinyl ether system was selected.[4b]

An exhaustive exploration of the potential energy surfaces (PESs) allows us to find also several molecular complexes (MCs) associated with the early stages of these cycloadditions and situated on a very flat region that control the access to the different reactive channels. The formation of these MCs may take place in different arrangements of the reactants, with a large distance between the diene and dienophile fragments (3.3–3.5 Å) which correspond to van der Waals complexes.[4b] Their presence on a very flat surface on the PES makes the location of the MC associated with each reactive channel very difficult. Therefore, the more stable MCs, **MC-X**, are considered. The formation of these species takes place without an appreciable barrier; the MCs are between 4.6 and 7.4 kcal mol^{-1} (1 kcal = 4.184 kJ) more stable than the isolated reactants **R1-X** and **R2** (see Table 1).

Analysis of the results shows that these LA-catalyzed cycloadditions are two-stage processes, which are concerted but not synchronous.[22,23] Only the C—C bond is being formed in the first half of the reaction as a consequence of the nucleophilic attack of the β-position of the vinyl ether, C5 position, to the conjugated position of the nitroethene, C4 position. Therefore, on going from the molecular complexes to the corresponding TSs, these nucleophilic attacks are one-center additions instead of two-center additions associated with [4 + 2] processes.

The values of the relative energies with respect to separate reactants for **TS-en-X** and **TS-ex-X** are 1.1 and 1.7 kcal mol^{-1} (for **X** = Me), −3.9 and −3.6 kcal mol^{-1} (for **X** = OMe) and −5.9 and −5.8 kcal mol^{-1} (for **X** = Cl), respectively. However, if we consider the formation of the molecular complexes, **MC-X**, the potential energy barriers (PEBs) become all positive (see Table 1). For the cycloaddition using $Al(OMe)_3$ and $AlCl_3$ there is an inverted energy profile and the corresponding values of the barrier heights are between

Table 1. B3LYP/6–31G* total energies (au) and relative energies[a] (kcal mol^{-1}, in parentheses) for the stationary points corresponding to the LA aluminum-catalyzed cycloadditions between nitroethene **R1** and methyl vinyl ether **R2**, *in vacuo* and in dichloromethane

	In vacuo		In dichloromethane	
R2	−193.110423		−193.1122647	
R1-Me	−645.297957		−645.304398	
MC-Me	−838.415768	(−4.64)	−838.421350	(−2.94)
TS-en-Me	−838.406630	(1.10)	−838.416974	(−0.20)
TS-ex-Me	−838.405623	(1.73)	−838.414216	(1.54)
P-en-Me	−838.459749	(−32.23)	−838.469698	(−33.28)
R1-OMe	−871.074725		−871.084517	
MC-OMe	−1064.196981	(−7.43)	−1064.205102	(−5.22)
TS-en-OMe	−1064.191433	(−3.94)	−1064.204774	(−5.01)
TS-ex-OMe	−1064.190943	(−3.64)	−1064.203222	(−4.04)
P-en-OMe	−1064.243792	(−36.80)	−1064.256180	(−37.27)
R1-Cl	−1906.360753		−1906.372394	
MC-Cl	−2099.482514	(−7.11)	−2099.493079	(−5.28)
TS-en-Cl	−2099.480553	(−5.88)	−2099.496015	(−1.84)
TS-ex-Cl	−2099.480369	(−5.77)	−2099.492593	(2.15)
P-en-Cl	−2099.534170	(−39.53)	−2099.550341	(−36.24)

[a] Relative to **R1-X** + **R2**.

1.2 and 5.7 kcal mol^{-1}, respectively. All reactions are exothermic processes, in the range −32.2 to −39.5 kcal mol^{-1}. **P-en-X** and **P-ex-X** are a pair of enantiomers with the same energy.

Analysis of the relative energies indicates that there is a reduction of the barrier associated with the electron-withdrawing character of the substituent present on the aluminum metal that increases the acidic character of the aluminum salt: Me < OMe < Cl (see the next section). The *endo* TSs, **TS-en-X**, are between 0.1 and 0.6 kcal mol^{-1} more stable than the *exo* TSs, **TS-ex-X**. Therefore, in the gas phase these cycloadditions present a low *endo* selectivity that decreases with the reduction of the barrier. These PEBs are between 7 and 12 kcal mol^{-1} lower than those for the uncatalyzed process; the PEB for the **R1** + **R2** DA reaction is 13.5 kcal mol^{-1}.[4b] Therefore, this lowering of the activation energy indicates a large catalytic effect on these LA-catalyzed cycloadditions in agreement with the reaction conditions. Some of these catalyzed cycloadditions were carried out at very low temperature, −78 °C.[24] Finally, the **R1**-$AlMe_3$/**R2** cycloaddition presents a similar barrier to that found for the **R1**-BH_3/**R2** reaction model, 7.5 kcal mol^{-1}.[4b]

Geometries, bond orders and charge transfer analysis

The lengths of the C4—C5 and O1—C6 forming bonds at the *endo* TSs are 2.094 and 2.781 Å for **TS-en-Me**, 2.191 and 2.834 Å for **TS-en-OMe** and 2.267 and 2.972 Å for **TS-en-Cl**, respectively, whereas for the *exo* TSs these lengths are 2.141 and 2.688 Å for **TS-en-Me**, 2.342 and 2.844 Å for **TS-en-OMe**, and 2.404 and 2.917 Å for **TS-en-Cl**, respectively. These lengths indicate that these TSs correspond to high asynchronous bond formation processes where the C4—C5 is more advanced than the O1—C6 bond formation. The *endo* TSs are more asynchronous than the *exo* TSs. In addition, on going through the series Me, OMe, Cl the process becomes earlier. The TSs associated with the $AlMe_3$-catalyzed cycloaddition present a similar bond formation to that found for the BH_3-catalyzed cycloaddition.[4b] The Al—O8 lengths in the *endo* TSs are 2.023, 1.952 and 1.912 Å, respectively. Similar results are found for the *exo* TSs. In consequence, there is a decrease in the Al—O8 bond lengths with increase in the electron-withdrawing character of the substituent on the aluminum metal.

The extent of bond formation along a reaction pathway is provided by the concept of bond order (BO).[25] The BO values of the C4—C5 and O1—C6 forming bonds at the *endo* TSs are 0.42 and 0.07 for **TS-en-Me**, 0.35 and 0.06 for **TS-en-OMe**, and 0.31 and 0.05 for **TS-en-Cl**, respectively, and for the *exo* TSs these values are 0.34 and 0.08 for **TS-ex-Me**, 0.28 and 0.05 for **TS-ex-OMe** and 0.24 and 0.05 for **TS-ex-Cl**, respectively. These BO values indicate highly asynchronous TSs where only the C4—C5 bond is being formed on going from **MC-X** to TSs. Therefore, these TSs correspond to one-center additions instead of [4 + 2] processes. The C6—O7 BO values at the *endo* TSs are ca 1.15, indicating a slight π character for the C6—O7 bond as a consequence of the participation of the O7 lone pair in the nucleophilic attack of MVK on **R1-X**.

These two-stage reactions[22] are supported by an analysis of the evolution of the bond formation from the TSs to the cycloadducts along the IRC paths for these concerted processes.[23] Thus, the geometries of the points at 'half way' between the saddle point **TS-en-Me** and the cycloadduct **P-en-Me** show that whereas the C4—C5 bond formation is very advanced, the C4—C5 bond lengths at these points are ca 1.6 Å, the O1—C6 bond formation is very delayed and the O1—C6 distance remain at 2.60 Å. Moreover, these points are located in a smooth drop in energy after the barrier height, thus explaining the failure to locate the corresponding zwitterionic acyclic intermediate as a stationary point.[23]

Finally, the natural population analysis[14a] allows us to evaluate the charge transferred along the cycloaddition process. The B3LYP/6–31G* atomic charges at the TSs are shared between the donor vinyl ether **R2** and the acceptor LA-coordinated nitroethene **R1-X**. The values of the charge transferred from **R2** to **R1-X** at the *endo* TSs are 0.37 e (**TS-en-Me**), 0.33 e (**TS-en-OMe**) and 0.33 e (**TS-en-Cl**), and those for the *exo* TSs are 0.34 e (**TS-ex-Me**), 0.29 e (**TS-ex-OMe**) and 0.28 e (**TS-ex-Cl**), indicating that the nature of these TSs can be seen to involve some zwitterionic character.[4b] In addition, the charge transfer is slightly larger for the more favorable *endo* TSs than for the *exo* TSs. For the $AlMe_3$-catalyzed cycloaddition, the charge transfer is similar to that found for the **R1**-BH_3-catalyzed process.[4b]

Since these TSs present similar charge transfer, the charges on the acceptor residue, **R1-X**, are shared between the nitroethene and the LA frameworks in order to explain the substitution effect on the aluminum metal. Thus, the negative charge raised in the nitroethene framework at the TSs is 0.22 e at **TS-en-Me**, 0.19 e at **TS-en-OMe** and 0.15 e at **TS-en-Cl**. There is a decrease in the negative charge on the nitroethene framework with increase in the electron-withdrawing character of the substituent on the aluminum. Therefore, the delocalization of the negative charge that is being transferred during the nucleophilic attack of MVK to **R1-X** is responsible for the reduction in activation energy of the cycloaddition.[21c]

A comparison of the relative energies, geometric parameters and charge transfer between the BH_3- and $AlMe_3$-catalyzed cycloadditions indicates that both computational models describe a similar bond-formation process. In consequence, we found that the small BH_3 molecule is a valuable computational model for the study of LA-catalyzed cycloadditions based on aluminum metal.[26]

Table 2. Global properties of nitroethene **R1**, Lewis acid-coordinated nitroethenes, **R1**-LA, and methyl vinyl ether, **R2**

Molecule	μ (au)	η (au)	ω (ev)
R1-$AlCl_3$	−0.2323	0.1124	6.53
R1-$Al(OMe)_3$	−0.1900	0.0869	5.65
R1-$AlMe(OMe)_2$	−0.1868	0.0856	5.55
R1-$AlMe_3$	−0.1830	0.0825	5.52
R1-AlH_3	−0.2032	0.1083	5.19
R1-BH_3	−0.2047	0.1317	4.33
R1	−0.1958	0.2001	2.61
R2	−0.0894	0.2564	0.42

Study of the solvent effects on the LA aluminum-catalyzed cycloadditions

Recent studies carried out on LA-catalyzed cycloaddition reactions indicate that the inclusion of the solvent effects on the geometry optimization does not modify the gas-phase geometries substantially.[4] In consequence, solvent effects were considered by single-point calculations for the gas-phase optimized geometries using a relatively simple SCRF method,[16] based on the PCM method of Tomasi's group.[17] Table 1 reports the total and relative energies of the stationary points in dichloromethane, $\varepsilon = 8.93$.

Inclusion of solvent effects leads to stabilization of the LA-coordinated structures of between 4 and 10 kcal mol^{-1} due to the high polar character of these species. A different behavior is found with the inclusion of the solvent effect on the barriers associated with these catalyzed cycloadditions. Thus, whereas **TS-en-Me** and **TS-en-OMe** present lower barriers than in the gas phase, ca 3.0 and 3.3 kcal mol^{-1}, respectively, for **TS-en-Cl** there is an increase of ca 2.3 kcal mol^{-1} due to a preferential solvation of the molecular complex **MC-Cl**.

A more relevant effect with the inclusion of dichloromethane as a continuum model is the increase in the *endo* selectivity for these LA-catalyzed reactions relative to that obtained in the gas phase (see Table 1). This behavior is due to a preferential solvation of the more polar *endo* TSs over their corresponding *exo* counterparts (see NPA analysis and Ref. 4b). This is in qualitative agreement with the increase in the *endo/exo* selectivity with the polarity of the solvent experimentally observed for related reactions.[27]

Global electrophilicity analysis

These LA-catalyzed cycloadditions were also analyzed using the global indexes defined in the context of DFT.[18,19] Recent studies devoted to the Diels–Alder reaction have shown that these global indexes are a powerful tool for understanding the behavior of these polar cycloadditions.[20,21] Thus, the difference in global electrophilicity power[19] between the diene/dienophile pair, $\Delta\omega$, can be used to predict the polar character of the process and the feasibility of the cycloaddition.[20] In Table 2 the static global properties, electronic chemical potential μ, chemical hardness η and global electrophilicity ω for nitroethene, **R1**, six LA-coordinated nitroethenes, **R1**-LA [LA = BH_3, AlH_3, $AlMe_3$, $AlMe(OMe)_2$, $Al(OMe)_3$, $AlCl_3$] and MVE, **R2**, are given.

The electronic chemical potential of nitroethene **R1** ($\mu = -0.1958$ au) is less than that of MVE **R2** ($\mu = -0.0894$ au), indicating that the net charge transfer at the nitroethene + MVE cycloaddition will take place from **R2** towards **R1**, in agreement with the charge-transfer analysis, and with an IED reactivity.[4b] Nitroethene **R1** has a large electrophilicity power, $\omega = 2.61$ eV, and it has been classified as strong electrophile.[20] On the other hand, MVE **R2** has a very low electrophilicity power, $\omega = 0.42$ eV, so it has been classified as a marginal electrophile or a nucleophile.[20] In consequence, it is expected that the cycloaddition will have a large polar character, $\Delta\omega = 2.19$ eV. The presence of the BH_3 coordinated to nitroethene increases markedly the electrophilicity of the acceptor **R1**, as is shown by the high electrophilicity power calculated for the **R1**-BH_3 complex, $\omega = 4.33$ eV. This increase in electrophilicity for the LA-coordinated heterodiene enhances the electrophilicity difference for the **R1**-BH_3/**R2** pair, $\Delta\omega = 3.91$ eV, and in consequence increases the polar character of the cycloaddition.[20] Therefore, the enhancement of the electrophilicity for the **R1**-LA complexes is responsible for the reduction of the activation energy found at these LA-catalyzed processes.[4b,20,21c]

Substitution of boron for a more electropositive aluminum metal increases the electrophilicity power for the **R1**-AlH_3 complex, $\omega = 5.19$ eV, and in consequence the cycloaddition will have a more ionic character. In addition, substitution of the hydrogen atoms for more electronegative groups increases the electrophilicity of the corresponding complex. Thus, the increase in the electrophilicity power for the series **R1**-$AlMe_3$, $\omega = 5.52$ eV, **R1**-$Al(OMe)_3$, $\omega = 5.65$ eV, and **R1**-$AlCl_3$, $\omega = 6.53$ eV is in complete agreement with the lowering of the barriers found in gas phase (see earlier). Finally, Table 2 also gives the global parameters for the **R1**-$AlMe(OMe)_2$ complex, as a reduced model for the MAPh and MAD catalysts. The electrophilicity power for **R1**-$AlMe(OMe)_2$, $\omega = 5.55$ eV, is well positioned between the **R1**-$AlMe_3$ and **R1**-$Al(OMe)_3$ complexes, in agreement with an additive character of the substitution on the aluminum metal.

From this DFT analysis, we can conclude that the increase in the static electrophilicity power for the LA-coordinated heterodiene relative to the non-coordinated one allows us to explain the role of these LA catalysts. The use of a more electropositive metal, aluminum, instead of boron, or/and a more electron-withdrawing substituent, Me, OMe, and Cl, increases the electrophilicity power of the **R1**-LA complex. This substitution

enhances the $\Delta\omega$ of the diene–dienophile pair interaction, giving a more ionic process with a lower activation energy, in agreement with the experimental results.

CONCLUSIONS

The mechanism for the inverse electron demand Diels–Alder reaction of nitroethene with vinyl methyl ether catalyzed by Lewis acids based on aluminum, $AlMe_3$, $Al(OMe)_3$ and $AlCl_3$ was studied using DFT methods at the B3LYP/6–31G* computational level. For these cycloaddition reactions, two reactive channels corresponding to the *endo* and *exo* approach modes of the vinyl ether to the Lewis acid coordinated nitroethene were studied. These LA-catalyzed cycloadditions are concerted but non-synchronous processes, in which only the C—C bond is being formed in the first half of the reaction as a consequence of the nucleophilic attack of the vinyl ether on the conjugated position of the LA-coordinated nitroethene. Hence these LA-catalyzed cycloadditions are one-center additions instead of $[4 + 2]$ processes.

Coordination of the aluminum metal to an oxygen atom of nitroethene decreases markedly the activation energy of the cycloaddition caused by an increase in the electrophilicity of the heterodiene that increases the ionic character of the process. In addition, the presence of electron-withdrawing substituents on the aluminum increases the electrophilicity of the LA-coordinated nitroethene complex through a larger delocalization of the negative charge that is being transferred to nitroethene along these polar bond-formation processes. In the gas phase these cycloadditions present a low *endo* selectivity that is enhanced with the inclusion of solvent effects.

Finally, a DFT analysis of the electrophilicity of the reactants allows the behaviors of these LA catalysts based on aluminum metal to be explained. Coordination of the LA to nitroethene increases notably the electrophilicity of the heterodiene, increasing the $\Delta\omega$ of the diene–dienophile pair and decreasing the activation energy by an increase in the ionicity of the process.

Acknowledgements

This work was supported by research funds provided by the Ministerio de Educación y Cultura of the Spanish Government and by DGICYT (project PB98-1429). All calculations were performed on a Cray-Silicon Graphics Origin 2000 compute of the Servicio de Informática de la Universidad de Valencia. The authors are most indebted to this center for providing computer capabilities. P.A. thanks the Ministerio de Educación y Cultura for an FPU fellowship.

REFERENCES

1. (a) Carruthers W. *Some Modern Methods of Organic Synthesis* (2nd edn). Cambridge University Press: Cambridge, 1978; (b) Carruthers W. *Cycloaddition Reactions in Organic Synthesis*. Pergamon Press: Oxford, 1990.
2. (a) Kagan HB, Riant O. *Chem. Rev.* 1992; **92**: 1007; (b) Tietze LF, Kettschau G. *Top. Curr. Chem.* 1997; **189**: 1; (c) Fringuelli F, Piermatti O, Pizzo F, Vaccaro L. *Eur. J. Org. Chem.* 2001; 439.
3. (a) Loncharich R, Schwartz TR, Houk KN. *J. Am. Chem. Soc.* 1987; **109**: 14; (b) Gurner OF, Ottenbrite RM, Shillady DD, Alston PV. *J. Org. Chem.* 1987; **52**: 391; (c) Guner OF, Ottenbrite RM, Shillady DD, Alston PV. *J. Org. Chem.* 1987; **52**: 391; (d) Fox M, Cardona R, Kiwiet NJ. *J. Org. Chem.* 1987; **52**: 1469; (e) Houk KN, Loncharich RJ, Blake JF, Jorgensen WL. *J. Am. Chem. Soc.* 1989; **111**: 9172; (f) Loncharich RJ, Brown FK, Houk KN. *J. Org. Chem.* 1989; **54**: 1129; (g) Birney DM, Houk KN. *J. Am. Chem. Soc.* 1990; **112**: 4127; (h) Guner OF, Lammertsma K, Alston PV, Ottenbrite RM, Shillady DD. *J. Org. Chem.* 1990; **55**: 28; (i) Raimondi L, Brown FK, Gonzalez J, Houk KN. *J. Am. Chem. Soc.* 1992; **114**: 4796; (j) Gonzalez J, Houk KN. *J. Org. Chem.* 1992; **57**: 3031; (k) Sato K, Sakuma Y, Iwabuchi S, Hirai H. *J. Polym. Sci., Part A: Polym. Chem.* 1992; **30**: 2011; (l) Jorgensen WL, Lim D, Blake JF. *J. Am. Chem. Soc.* 1993; **115**: 2936; (m) McCarrick MA, Wu Y-D, Houk KN. *J. Org. Chem.* 1993; **58**: 3330; (n) Menéndez MI, González J, Sordo JA, Sordo TL. *J. Mol. Struct. (THEOCHEM)* 1994; **314**: 241; (o) De Pascual-Teresa B, Gonzalez J, Asensio A, Houk KN. *J. Am. Chem. Soc.* 1995; **117**: 4347; (p) Dai WM, Lau CW, Chung SH, Wu Y-D. *J. Org. Chem.* 1995; **60**: 8128; (q) González J, Sordo TL, Sordo JA. *J. Mol. Struct. (THEOCHEM)* 1996; **358**: 23; (r) Ishihara K, Kondo S, Kurihara H, Yamamoto H, Oshashi S, Inagaki S. *J. Org. Chem.* 1997; **62**: 3026; (s) Sbai A, Branchadell V, Ortuño RM, Oliva A. *J. Org. Chem.* 1997; **62**: 3049; (t) García JI, Mayoral JA, Salvatella L. *Tetrahedron* 1997; **53**: 6057; (u) García JI, Martínez-Merino V, Mayoral JA, Salvatella L. *J. Am. Chem. Soc.* 1998; **120**: 2415; (v) Tietze LF, Schuffenhauer A, Schreiner PR. *J. Am. Chem. Soc.* 1998; **120**: 7952; (w) Singleton DA, Merrigan SR, Beno BR, Houk KN. *Tetrahedron Lett.* 1999; **40**: 5817; (x) Yamabe S, Minato T. *J. Org. Chem.* 2000; **65**: 1830; (y) Alves CN, da Silva ABF, Martí S, Moliner V, Oliva M, Andrés J, Domingo LR. *Tetrahedron* 2002; **58**: 2695.
4. (a) Domingo LR, Picher MT, Andrés J. *J. Phys. Org. Chem.* 1999; **12**: 24; (b) Domingo LR, Arnó M, Andrés J. *J. Org. Chem.* 1999; **64**: 5867; (c) Domingo LR, Asensio A. *J. Org. Chem.* 2000; **65**: 1076.
5. Denmark SE, Thorarensen A. *Chem. Rev.* 1996; **96**: 137.
6. Cativiela C, Dillet V, García JI, Mayoral JA, Ruiz-López MF, Salvatella L. *J. Mol. Struct. (THEOCHEM)* 1995; **331**: 37.
7. (a) Parr RG, Yang W. *Density Functional Theory of Atoms and Molecules*. Oxford University Press: New York, 1989; (b) Ziegler T. *Chem. Rev.* 1991; **91**: 651.
8. (a) Becke AD. *J. Chem. Phys.* 1993; **98**: 5648; (b) Lee C, Yang W, Parr RG. *Phys. Rev. B* 1988; **37**: 785.
9. Hehre WJ, Radom L, Schleyer PvR, Pople JA. *Ab initio Molecular Orbital Theory*. Wiley: New York, 1986.
10. (a) Schlegel HB. *J. Comput. Chem.* 1982; **3**: 214; (b) Schlegel HB. Geometry Optimization on Potential Energy Surface. In *Modern Electronic Structure Theory*, Yarkony DR (ed). World Scientific Publishing: Singapore, 1994.
11. Tapia O, Andrés J. *Chem. Phys. Lett.* 1984; **109**: 471.
12. Fukui K. *J. Phys. Chem.* 1970; **74**: 4161.
13. (a) González C, Schlegel HB. *J. Phys. Chem.* 1990; **94**: 5523; (b) González C, Schlegel HB. *J. Chem. Phys.* 1991; **95**: 5853.
14. (a) Reed AE, Weinstock RB, Weinhold F. *J. Chem. Phys.* 1985; **83**: 735; (b) Reed AE, Curtiss LA, Weinhold F. *Chem. Rev.* 1988; **88**: 899.
15. Frisch MJ, Trucks GW, Schlegel HB, Scuseria GE, Robb MA, Cheeseman JR, Zakrzewski VG, Montgomery JJA, Stratmann RE, Burant JC, Dapprich S, Millam JM, Daniels AD, Kudin KN, Strain MC, Farkas O, Tomasi J, Barone V, Cossi M, Cammi R, Mennucci B, Pomelli C, Adamo C, Clifford S, Ochterski J, Petersson GA, Ayala PY, Cui Q, Morokuma K, Malick DK, Rabuck AD, Raghavachari K, Foresman JB, Cioslowski J, Ortiz JV, Stefanov BB, Liu G, Liashenko A, Piskorz P, Komaromi I, Gomperts R,

Martin RL, Fox DJ, Keith T, Al-Laham MA, Peng CY, Nanayakkara A, Gonzalez C, Challacombe MW Gill PM, Johnson B, Chen W, Wong MW, Andres JL, Gonzalez C, Head-Gordon M, Replogle ES, Pople JA. *Gaussian 98, Revision A.6*. Gaussian: Pittsburgh, PA, 1998.
16. (a) Tapia O. *J. Math. Chem.* 1992; **10**: 139; (b) Tomasi J, Persico M. *Chem. Rev.* 1994; **94**: 2027; (c) Simkin BY, Sheikhet I. *Quantum Chemical and Statistical Theory of Solutions–A Computational Approach*. Ellis Horwood: Chichester 1995.
17. (a) Cances MT, Mennunci V, Tomasi J. *J. Chem. Phys.* 1997; **107**: 3032; (b) Cossi M, Barone V, Cammi R, Tomasi J. *Chem. Phys. Lett.* 1996; **255**: 327; (c) Barone V, Cossi M, Tomasi J. *J. Comput. Chem.* 1998; **19**: 404.
18. Parr RG, Pearson RG. *J. Am. Chem. Soc.* 1983; **105**: 7512.
19. Parr RG, von Szentpaly L, Liu S. *J. Am. Chem. Soc.* 1999; **121**: 1922.
20. Domingo LR, Aurell MJ, Pérez P, Contreras R. *Tetrahedron*, 2002; **58**: 4417.
21. (a) Domingo LR, Arnó M, Contreras R, Pérez P. *J. Phys. Chem. A* 2002; **106**: 952; (b) Domingo LR, Aurell MJ. *J. Org. Chem.* 2002; **67**: 959; (c) Domingo LR. *Tetrahedron* 2002; **58**: 3765.
22. Dewar MJS, Olivella S, Stewart JJP. *J. Am. Chem. Soc.* 1986; **108**: 5771.
23. Domingo LR. *J. Org. Chem.* 2001; **66**: 3211.
24. Denmark SE, Middleton DS. *J. Org. Chem.* 1998; **63**: 1604.
25. Wiberg KB. *Tetrahedron* 1968; **24**: 1083.
26. Domingo LR. *Eur. J. Org. Chem.* 2000; 2265.
27. Cativiela C, García JI, Mayoral JA, Salvatella L. *Chem. Soc. Rev.* 1996; **25**: 209.

